

# NOVEL ALGORITHM FOR HIGH RESOLUTION PASSIVE RADAR IMAGING WITH ISDB-T DIGITAL TV SIGNAL

<sup>1</sup>Weike Feng, Student member, IEEE, <sup>2,3</sup>Jean-Michel Friedt, <sup>1</sup>Grigory Cherniak, and <sup>2</sup>Motoyuki Sato, Fellow, IEEE

<sup>1</sup>Graduate School of Environmental Studies, Tohoku University, Sendai, Japan

<sup>2</sup>Center for Northeast Asian Studies, Tohoku University, Sendai, Japan

<sup>3</sup>FEMTO-ST, Time & Frequency department, Besancon, France

E-mail: feng.weike.q4@dc.tohoku.ac.jp, motoyuki.sato.b3@tohoku.ac.jp

## ABSTRACT

We have studied passive radar with digital broadcasting terrestrial signals for imaging moving and stationary targets. We combined multiple TV channels to improve the range resolution. In order to reduce the high-level sidelobes caused by the frequency gaps among multiple channels, a low rank matrix completion based method is proposed. We present the experiment results of range-Doppler mapping of moving targets, high-resolution time delay estimation, and passive synthetic aperture radar (SAR) imaging of stationary targets. It is shown that, by the designed system, a landing airplane can be detected and tracked. By combining multiple TV channels, high resolution time delay estimation can be achieved. Buildings located within 55 meters can be effectively imaged by the proposed method.

**Index Terms**— Passive radar, synthetic aperture radar, ISDB-T, low rank matrix completion

## 1. INTRODUCTION

Passive bistatic radar using non-cooperative illuminators has drawn attentions during the last decades [1]. Compared with active radar, passive radar has smaller vulnerability and EM interferences. Digital terrestrial television broadcasting (DTTB) signal has been extensively studied due to its attractive ambiguity function, urban-wide coverage, high transmitted power, and continuous emission [2]. In Japan, Integrated Services Digital Broadcasting Terrestrial (ISDB-T) is used as the DTTB standard, and some passive radar studies adopting ISDB-T signal have been conducted [3].

Various signal processing techniques have been proposed for passive radar. For example, an efficient algorithm for moving target range-Doppler map formation is presented in [2]. Based on compressive sensing (CS) theory, passive inverse SAR (ISAR) imaging is studied in [4]. Passive radar direction finding via an Adcock antenna array is proposed in [5]. Recently, some studies of airborne

passive SAR imaging are performed and pioneering experimental results are presented [6].

We have studied passive radar with ISDB-T signal for target imaging [7]. We combined multiple TV channels to obtain sufficient bandwidth for high range resolution. We observed that the frequency gaps among multiple TV channels cause high-level sidelobes in the range direction. To solve this problem, we propose a low rank matrix completion (MC) [8], [9] based method in this paper.

## 2. MOVING TARGETS DETECTION

In order to evaluate the target detection capacity of passive radar using ISDB-T signal, whose spectrum is shown in Fig. 1, range-Doppler mapping of moving targets was studied. Two low-cost commercial DVB-T receivers clocked by a common clock are used to provide long integration time for enough Doppler resolution. The 2D cross-ambiguity function is calculated to estimate the range and Doppler frequencies of moving targets, given as

$$\chi(\tau, f_d) = \int_0^{T_{int}} s_{sur}(t) s_{ref}^*(t - \tau) e^{-j2\pi f_d t} dt \quad (1)$$

where  $s_{ref}(t)$  and  $s_{sur}(t)$  are the reference and measurement signals,  $(\cdot)^*$  denotes the complex conjugate,  $\chi(\tau, f_d)$  is the range-Doppler map of targets,  $\tau$  and  $f_d$  are the expected time delay and Doppler frequency of the target. We used the batches algorithm proposed in [2] to calculate (1) efficiently.

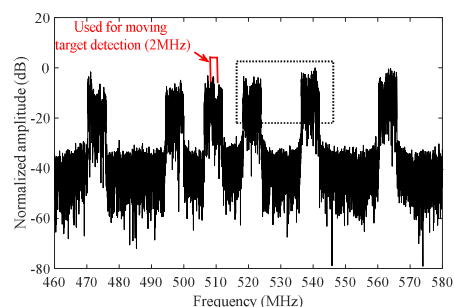


Fig. 1. Spectrum of ISDB-T signal in Sendai.

We carried out range-Doppler mapping experiments with two Yagi-Uda antennas to observe a landing airplane using a 2-MHz frequency bandwidth, as shown in Fig. 2. Since the direct path interference and stationary targets have small changes in different batches, we employed mean-value subtraction to suppress their influences. The tracking result of the landing airplane in range-Doppler domain during 1 min record is shown in Fig. 3.



Fig. 2. Landing airplane detection and tracking experiment.

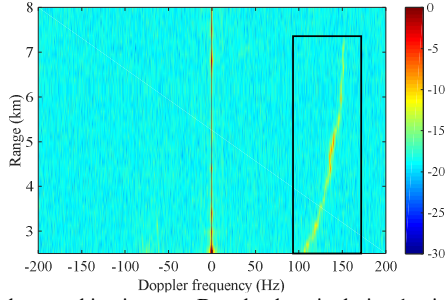


Fig. 3. Airplane tracking in range-Doppler domain during 1-minute record.

### 3. TIME DELAY ESTIMATION

Although low-cost DVB-T receivers can be used for moving target detection, low sampling rate makes it unsuitable for high range resolution passive radar imaging. Therefore, we use a digital oscilloscope, which has a higher data sampling rate, to sample multiple TV channels to improve the range resolution. Six digital TV channels using ISDB-T are broadcast in Sendai from three TV towers, whose assigned frequencies are from 470 MHz to 570 MHz, as shown in Fig. 1. Four channels are emitted from one TV tower, while the other two channels, which are indicated by the dotted rectangle in Fig. 1, are emitted from the other two towers. In current research, we use three channels (473, 497, and 509 MHz) for passive radar imaging. As the fundamental research stage, by conducting the time delay estimation experiments, we tested the capability of multiple TV channels used as the sources for passive radar imaging. Without considering the multipath echoes, the reference signal is given by

$$s_{ref}(t) = A_{ref}s_0(t - t_{ref}) + n_{ref}(t) \quad (2)$$

where  $s_0(t)$  is the transmitted signal,  $A_{ref}$  is the amplitude,  $t_{ref}$  is the time delay of the reference signal, and  $n_{ref}(t)$  is the noise. Similarly, the measurement signal is given by

$$s_{sur}(t) = A_{sur}s_0(t - t_{sur}) + n_{sur}(t) \quad (3)$$

where  $A_{sur}$  is the amplitude of the measurement signal with time delay  $t_{sur}$ , and  $n_{sur}(t)$  is the noise.

Time delay between two signals is calculated by cross-correlation [1], which can be implemented by the fast Fourier transform (FFT) as

$$\tilde{\chi} = F^H s(\mathbf{f}) = F^H [s_{sur}(\mathbf{f}) \odot s_{ref}^*(\mathbf{f})] \quad (4)$$

where  $F$  is the Fourier transform matrix,  $\odot$  denotes the element-wise multiplication,  $(\cdot)^H$  is the conjugate transpose,  $s_{ref}(\mathbf{f})$  and  $s_{sur}(\mathbf{f})$  are the reference and measurement signals in frequency domain.

Time delay estimation results obtained by direct cross-correlation are shown in Fig. 4 for several different distances between two antennas. It is observed that, although the time delay can be accurately estimated with high resolution, due to the frequency gaps between three used TV channels, the results have high-level sidelobes. When applied to passive SAR imaging, the high-level sidelobes of strong targets will blur the weaker targets.

Recently, MC has been proposed to recover a low rank matrix from its small set of corrupted entries. Compared with CS used in [4], MC can be used to reconstruct the missing data without designing an accurate dictionary. We introduce the MC algorithm to passive radar for predicting the data of missing frequencies. Consider the frequency domain signal vector  $s(\mathbf{f})$  in (4), given by

$$s(\mathbf{f}) = s_{sur}(\mathbf{f}) \odot s_{ref}^*(\mathbf{f}) = \alpha \exp(-j2\pi\mathbf{f}\tau_0) + \mathbf{n} \quad (5)$$

and rearrange it as a matrix

$$\mathbf{S} = \alpha [e^{-j2\pi f_1 \tau_0}, \dots, e^{-j2\pi f_P \tau_0}]^T [1, \dots, e^{-j2\pi f_{(Q-1)P} \tau_0}] + \mathbf{N} \quad (6)$$

where  $\tau_0 = t_{sur} - t_{ref}$  is the time delay between two signals, the number of frequencies  $\mathbf{f}$  is  $M$ , and  $QP = M$ .

It can be learned that  $\mathbf{S}$  is a noise corrupted rank-one matrix. However, MC theory cannot directly be applied to recover the missing data of  $\mathbf{S}$ , which has fully missing columns caused by the continuous missing frequencies. Fortunately, by rearranging the original signal matrix  $\mathbf{S}$  as a matrix  $\mathbf{S}_{hankel}$  with a Hankel structure [9], MC theory can be applied to estimate the gapped frequency component, expressed as

$$\min \|\mathbf{S}_{hankel}\|_* \quad s.t. \quad \|\mathbf{P}_{\Omega}^{hankel}(\mathbf{S}_{hankel} - \mathbf{S}_{hankel}^0)\|_F \leq \epsilon_{hankel} \quad (7)$$

where  $\|\cdot\|_*$  denotes the nuclear norm of a matrix,  $\epsilon_{hankel}$  is the noise level,  $\mathbf{S}_{hankel}^0$  is the Hankel structured received signal matrix, and  $\mathbf{P}_{\Omega}^{hankel}$  indicates the positions of the frequencies within three used TV channels in structured Hankel form. In our current study, inexact augmented Lagrange multiplier algorithm [10] is used to solve (7).

After obtaining  $\mathbf{S}_{hankel}$ , matrix  $\mathbf{S}$  and vector  $s$  can easily be reconstructed. Then, the time delay can be estimated by  $\chi = F^H s$ . With the proposed frequency gaps filling method,

the spectrum of the received signal is shown in Fig. 5, and the estimated time delays are shown in Fig. 6, where the sidelobes have been reduced by about 10 dB compared with Fig. 4.

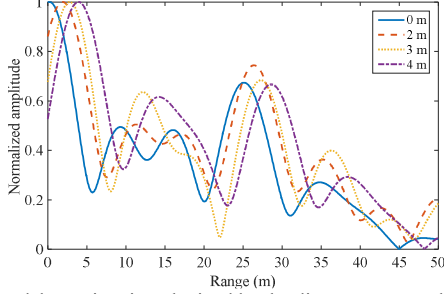


Fig. 4. Time delay estimation obtained by the direct cross correlation.

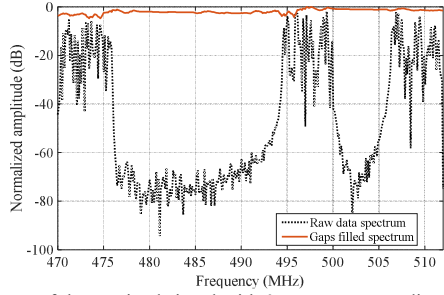


Fig. 5. Spectra of the received signal with 0-meter antenna distance.

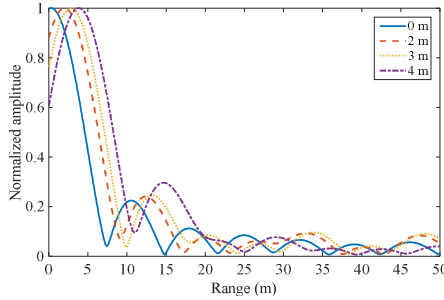


Fig. 6. Time delay estimation obtained after the gapped frequencies filling.

#### 4. PASSIVE SAR IMAGING

Based on the studies of moving target detection and time delay estimation, passive SAR experiments were conducted for stationary target imaging. In this case, two Yagi-Uda antennas are fixed at a positioner, and at each position, we used a digital oscilloscope to measure the data. At  $l$ -th position  $(x_l, 0)$ , the reference signal is expressed as

$$s_{ref}^l(t) = A_{ref}^l s_0(t - t_{ref}^l) + n_{ref}^l(t) \quad (8)$$

and the measurement signal is modeled as

$$s_{sur}^l(t) = A_{sur}^l s_0(t - t_{sur}^l) + \sum_{i=1}^I \alpha_i s_0(t - t_i^l) + n_{sur}^l(t) \quad (9)$$

where  $A_{sur}^l s_0(t - t_{sur}^l)$  denotes the direct-path interference received by the measurement antenna,  $\alpha_i$  and  $t_i^l$  are the reflection coefficient and time delay of the  $i$ -th target, and  $I$  is the number of targets.

The first step of passive SAR imaging is to suppress the strong direct-path interference in the measurement channel. In this paper, the extensive cancellation algorithm [11] is used for its simplicity and effectiveness. Then, the cross-correlation process can be conducted to get the  $l$ -th compressed range profile, giving

$$\mathcal{X}^l = \mathbf{F}^H \mathbf{s}^l(f) = \mathbf{F}^H [\tilde{s}_{sur}^l(f) \odot s_{ref}^l(f)^*] \quad (10)$$

Finally, SAR image of the targets can be obtained by applying the back-projection algorithm, given as

$$\tilde{\alpha}(r, \theta) = \sum_{l=1}^L \mathcal{X}^l (2\sqrt{(x_l - r \sin \theta)^2 + (r \cos \theta)^2} / c) \quad (11)$$

where  $\tilde{\alpha}(r, \theta)$  is the estimated amplitude of the point at  $(r, \theta)$ .

However, directly conducting cross-correlation will cause high-level sidelobes in range direction. When  $r_i > 2L^2/\lambda$ , the time delay of the  $i$ -th target at  $(r_i, \theta_i)$  can be approximated by  $\tau_i^l = 2(r_i - x_l \sin \theta_l) / c$ , resulting in

$$\mathbf{S}(m, l) \approx \sum_{i=1}^I \alpha_i e^{-j2k_m r_i} e^{j4\pi x_l \sin \theta_l / \lambda} + \mathbf{N}(m, l) \quad (12)$$

where  $\mathbf{S}$  is the received signal matrix,  $k_m = 2\pi f_m / c$  is the  $m$ -th wavenumber. Thus, the received signal matrix is given by

$$\mathbf{S}_{M \times L} \approx \mathbf{A}_{M \times I} \mathbf{A}_{I \times L} \mathbf{B}_{I \times L}^T + \mathbf{N}_{M \times L} \quad (13)$$

where  $\mathbf{A} = [\mathbf{a}_1, \dots, \mathbf{a}_I]$  with  $\mathbf{a}_i = [e^{-j2k_m r_i}, \dots, e^{-j2k_M r_i}]^T$ ,  $\mathbf{B} = [\mathbf{b}_1, \dots, \mathbf{b}_I]$  with  $\mathbf{b}_i = [e^{j4\pi x_l \sin \theta_l / \lambda}, \dots, e^{j4\pi x_L \sin \theta_l / \lambda}]^T$ , and  $\mathbf{A} = \text{diag}\{\alpha_1, \dots, \alpha_I\}$ .

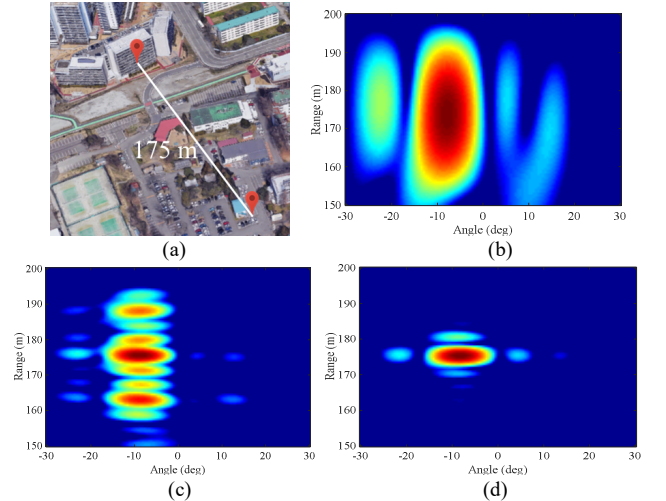


Fig. 7. (a) Experiment site and the imaged building, and reconstructed images of the building obtained (b) with 1 channel, (c) with 3 channels, and (d) after filling the frequency gaps of 3 channels.

Considering that some frequency components are missing in the received signal,  $\mathbf{A}$  is changed to  $\mathbf{A}^l = [\mathbf{a}_1^l, \dots, \mathbf{a}_I^l]$ , where  $\mathbf{a}_i^l = [e^{-j2k_m r_i}, \dots, \theta, \dots, e^{-j2k_M r_i}]^T$ , and  $\theta$  indicates the missing frequencies. Thus, the signal is changed to  $\mathbf{S}_{M \times L}^l \approx \mathbf{A}_{M \times I}^l \mathbf{A}_{I \times L} \mathbf{B}_{I \times L}^T + \mathbf{N}_{M \times L}$ . Then, the received signal matrix can be rearranged as a matrix  $\mathbf{S}_{st}$  with two-fold Hankel structure [9]. According to the theory of structured MC,  $\text{rank}(\mathbf{S}_{st}) \leq \text{rank}(\mathbf{A}_{I \times L}^l) = I$ . In such case, although the rank of  $\mathbf{S}_{st}$  is still bounded by the number of targets, the full-rows missing problem of  $\mathbf{S}$  usually

disappears. Therefore, by rearranging the measured signal  $\mathbf{S}^1$  as the two-fold Hankel structure, the missing data can be recovered by solving the following optimization problem.

$$\min \|\mathbf{S}_{st}\|_* \quad s.t. \quad \|\mathbf{P}_{\Omega, st}(\mathbf{S}_{st}^1 - \mathbf{S}_{st})\|_F \leq \epsilon_{st} \quad (14)$$

At last, rearranging the recovered structured matrix to its original form, SAR image can be obtained by

$$\tilde{\mathbf{A}} = \mathbf{F}_1^H \tilde{\mathbf{S}} \mathbf{F}_2^* \quad (15)$$

where  $\tilde{\mathbf{S}}$  is the frequency gaps filled signal matrix,  $\mathbf{F}_1$  is the Fourier transform matrix in range direction, and  $\mathbf{F}_2$  is the inverse Fourier transform matrix in azimuth direction.

With 2 Gsamples/s data sampling rate, 0.1 m moving step, and 2 m synthetic aperture, the reconstructed images of a building, which is located at about 175-meter away from the experiment site, are shown in Fig. 7 with dynamic range 20 dB. It can be learned from Fig. 7 (b) that, with only one TV channel which has the bandwidth 6 MHz, the resolution of the reconstructed image is poor. When three TV channels are used, since the frequency bandwidth is increased, the range resolution can be improved, as shown in Fig. 7 (c). However, strong sidelobes are produced by the frequency gaps. After filling the frequency gaps by the proposed method, we can effectively suppress the sidelobes and improve the imaging quality, as shown in Fig. 7 (d) and Fig. 8.

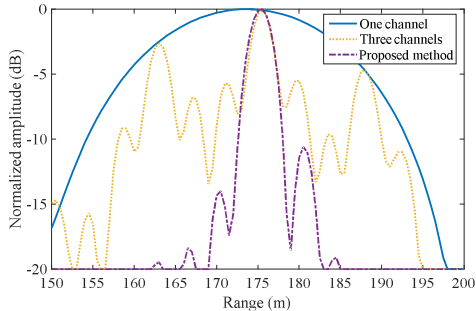


Fig. 8. Performance comparison in range direction.

We further validated the proposed passive SAR imaging method by using another building as a target, as shown in Fig. 9 (a). The reconstructed image is shown in Fig. 9 (b), where the building is well focused.

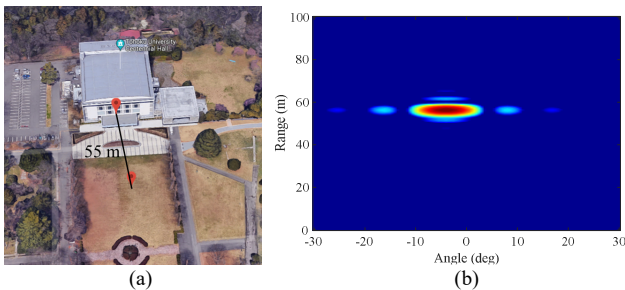


Fig. 9. (a) Experiment site and the imaged building located at about 55 m, and (b) reconstructed images of the building obtained after filling the frequency gaps of 3 channels.

## 5. CONCLUSION

Passive radar imaging using ISDB-T signal is studied in this paper. A low rank matrix completion based gapped frequencies filling method is proposed and validated using real data. Experiment results of moving targets detection and tracking, time delay measurement, and stationary targets SAR imaging demonstrate the imaging capacity of the designed passive radar system with ISDB-T signal.

## ACKNOWLEDGEMENTS

This work was supported by JSPS Grant-in-Aid for Scientific Research (A) 26249058.

## REFERENCES

- [1] J. Palmer, S. Palumbo, A. Summers, D. Merrett, S. Searle, and S. Howard, "An overview of an illuminator of opportunity passive radar research project and its signal processing research directions," *Digital Signal Processing*, vol. 21, no. 5, pp. 593–599, 2011.
- [2] C. Moscardini, D. Petri, A. Capria, M. Conti, M. Martorella, and F. Berizzi, "Batches algorithm for passive radar: A theoretical analysis," *IEEE Trans. Aerosp. Electron. Syst.*, vol. 51, no. 2, pp. 1475–1487, 2015.
- [3] J. Honda and T. Otsuyama, "Feasibility study on aircraft positioning by using ISDB-T signal delay," *IEEE Antennas Wireless Propag. Lett.*, vol. 15, pp. 1787–1790, 2016.
- [4] W. Qiu, E. Giusti, A. Bacci, M. Martorella, F. Berizzi, H. Zhao, and Q. Fu, "Compressive sensing-based algorithm for passive bistatic ISAR with DVB-T signals," *IEEE Trans. Aerosp. Electron. Syst.*, vol. 51, no. 3, pp. 2166–2180, 2015.
- [5] J. Wang, H.-T. Wang, and Y. Zhao, "Direction finding in frequency modulated-based passive bistatic radar with a four-element adcock antenna array," *IET radar, sonar & navigation*, vol. 5, no. 8, pp. 807–813, 2011.
- [6] D. Gromek, K. Kulpa, and P. Samczynski, "Experimental results of passive SAR imaging using DVB-T illuminators of opportunity," *IEEE Geosci. Remote Sens. Lett.*, vol. 13, no. 8, pp. 1124–1128, 2016.
- [7] B. Yang, L. Zou, and M. Sato, "Fundamental experiment on passive bistatic radar imaging using TV broadcasting wave", *IEICE Technical Report*, EMT2016-4, pp.27-32, 2016.
- [8] E. J. Candès, and B. Recht, "Exact Matrix Completion via Convex optimization," *Foundations of Computational Mathematics*, vol. 9, no. 6, pp. 717–772, 2009.
- [9] Y. Chen, and Y. Chi, "Robust spectral compressed sensing via structured matrix completion," *IEEE Trans. Inf. Theory*, vol. 60, no. 10, pp. 6576–6601, 2014.
- [10] Z. Lin, M. Chen, and Y. Ma, "The augmented Lagrange multiplier method for exact recovery of corrupted low-rank matrices," arXiv preprint arXiv:1009.5055, 2010.
- [11] F. Colone, R. Cardinali, and P. Lombardo, "Cancellation of clutter and multipath in passive radar using a sequential approach," in *Proceedings of IEEE International Conference on Radar*, 2006.